# Melatonin Enhances the Viability of Random-Pattern Skin Flaps by Activating the NRF2 pathway

**Keywords**
Melatonin, NRF2 pathway, Random-Pattern Skin Flaps

**Abstract**

Introduction
Random skin flap transplantation has been widely used in reconstructive and plastic surgery. As a well-known antioxidant, melatonin has the functions of eliminating reactive oxygen species (ROS), promoting angiogenesis, and protecting ischemia-reperfusion injury (IRI). We explored the effects of melatonin on random skin flap survival and the potential molecular mechanisms.

Material and methods
A total of 72 rats were randomly assigned to the control group, the melatonin (MEL) group, and MEL + ML385 groups. After the construction of random skin flap model, these groups were treated with physiological saline, melatonin, and melatonin + ML385. The general conditions of random skin flaps were observed daily after the procedure. Laser doppler blood flow imaging was used to evaluate the subcutaneous vascular network. On postoperative day 7, the animals were euthanized to obtain flap specimens. Hematoxylin-Eosin staining was used to evaluate the vessel density. Immunohistochemistry, immunofluorescence staining, and western blotting were used to evaluate the expression of proteins involved in angiogenesis, oxidative stress, and inflammation.

Results
Compared to the control group, the MEL group exhibited lower tissue water, more abundant vascular, and higher vascular density, thereby enhancing the survival of random flaps. Additionally, the MEL group showed increased expression of angiogenesis-related proteins, enhanced expression of antioxidant proteins, and decreased expression of inflammatory factors. Furthermore, ML385, reversed the beneficial effect of melatonin on random skin flaps.

Conclusions
These findings of our present study demonstrated that melatonin promotes angiogenesis, inhibits oxidative stress, and inflammation by activating NRF2 signaling pathway, thus the improving the survival of random skin flaps.

# Melatonin Enhances the Viability of Random-Pattern Skin Flaps by Activating the NRF2 pathway


## Abstract

**Background:** Random skin flap transplantation has been widely used in reconstructive and plastic surgery. As a well-known antioxidant, melatonin has the functions of eliminating reactive oxygen species (ROS), promoting angiogenesis, and protecting ischemia-reperfusion injury (IRI). We explored the effects of melatonin on random skin flap survival and the potential molecular mechanisms.

**Methods:** A total of 72 rats were randomly assigned to the control group, the melatonin (MEL) group, and MEL + ML385 groups. After the construction of random skin flap model, these groups were treated with physiological saline, melatonin, and melatonin + ML385, respectively. The general conditions of random skin flaps were observed daily after the procedure. Laser doppler blood flow (LDBF) imaging was used to evaluate the subcutaneous vascular network. On postoperative day 7, the animals were euthanized to obtain random skin flap specimens. Hematoxylin-Eosin (HE) staining was used to evaluate the vessel density. Immunohistochemistry, immunofluorescence staining, and western blotting were used to evaluate the expression of proteins involved in angiogenesis, oxidative stress, and inflammation.

**Results:** Compared to the control group, the MEL group exhibited lower tissue water content, a more abundant vascular network, and higher vascular density, thereby enhancing the survival of random skin flaps. Additionally, the MEL group showed increased expression of angiogenesis-related proteins, enhanced expression of antioxidant proteins, and decreased expression of inflammatory factors. Furthermore, ML385, a specific nuclear factor erythroid-2-related factor 2 (NRF2) inhibitor, reversed the beneficial effect of melatonin on random skin flaps.

**Conclusions:** These findings of our present study demonstrated that melatonin promotes angiogenesis, inhibits oxidative stress, and inflammation by activating

NRF2 signaling pathway, thus the improving the survival of random skin flaps.

**Key word:** Melatonin; Random-Pattern Skin Flaps; NRF2 pathway

## 1. Introduction

Random skin flaps have been widely used in plastic surgery to repair and reconstruct skin defects caused by trauma, pressure ulcers, tumor resection, diabetic wounds, and other factors(1, 2). The current treatment method is adversely affected by distal flap necrosis, limiting random skin flaps' application. After transplantation, random skin flaps may undergo severe ischemia due to the lack of axial vessels, and then neovascularization initiates from the flap pedicle toward the distal part. Subsequently, partial restoration and reperfusion of blood supply can lead to IRI(3). Recent studies have demonstrated that IRI-induced accumulation of ROS and inflammatory responses are important causes of skin flap necrosis(4, 5). In response to the mechanism of ischemic necrosis, various methods have been developed to promote the survival of random skin flaps. These methods include stimulating angiotsis, alleviating oxidative stress, and attenuating inflammation. Additionally, skin tissue engineering approaches based on novel hydrogels have also shown promising prospects(6, 7).

NRF2 is a transcription factor that activates a series of antioxidant genes and protects against xenobiotic and oxidative stress(8). Under stressful conditions, NRF2 dissociates from KEAP1 and translocates to the nucleus. Subsequently, NRF2 recognizes antioxidant response elements in the promoters of target genes, which include antioxidant enzymes and phase II detoxification enzymes, and triggers their expression(9). ML385 is a small-molecule, NRF2-specific inhibitor that binds to NRF2 and interferes with the DNA binding activity of the NRF2-MAFG protein complex, thereby inhibiting the expression of downstream target genes(10). Since excessive ROS can induce inflammation and cell death, NRF2-mediated anti-inflammatory effects may be based on ROS elimination. Previous studies have shown that inflammatory responses in NRF2-deficient mice can be suppressed by inhibiting ROS production(11). Furthermore, activation of NRF2 antioxidant defense system is

conducive to suppress oxidative stress and promote random skin flap survival(12). Altogether, these findings imply that drugs focused on modulating the NRF2 pathway could be an effective treatment for improving random skin flaps survival.

Melatonin is a pleiotropic hormone mainly synthesized and secreted by pineal gland and is involved in various physiological functions, including antioxidant(13), anti-inflammatory(14), immunomodulatory(15), neuroprotection(16), circadian rhythm regulation(17), oncostatic effects(18). Notably, recent studies have demonstrated that melatonin not only attenuates inflammatory responses by scavenging ROS, but also induces the activation of antioxidant enzymes via NRF2 signaling pathway(19). Furthermore, previous studies have shown that melatonin promotes angiogenesis by upregulating VEGF levels during the progression of osteoporotic bone defect repair and gastric ulcer healing(20, 21). Moreover, melatonin plays a protective role in IRI in many organs by reducing oxidative stress-induced cell damage(22, 23). Although studies have shown that melatonin can alleviate ischemic necrosis of random skin flaps, the molecular mechanism remains unclear.

Therefore, we hypothesized that melatonin might stimulate angiogenesis, attenuate oxidative stress and inflammation through the NRF2 signaling pathway, and improve random skin flap's survival. The aim of this study was to investigate the effect of melatonin on the survival of random skin flaps and to explore the related molecular mechanisms.



## 2. Materials and methods

### 2.1 Animals

Male Sprague-Dawley (SD) rats weighing 200-250g were purchased from the Laboratory Animal Center of our University (License No. SYXK [ZJ] 2020-0014). The rats were housed in single cages in an air-conditioned room with a temperature of 21-25℃, a humidity of 50-60%, and an alternating light / dark cycle every 12 hours. All animal experiments were performed following the Guide for the Care and Use of Laboratory Animals of National Institutes of Health in China, with the approval of the Institutional Animal Care and Use Committee of our University (xmsq 2022-0057).

## 2.2 Reagents and antibodies

Melatonin (purity: 99.73%, cat# 73-31-4) and ML385 (purity: 99.72%, cat# 846557-71-9) were obtained from MedChemExpress. The HE stain kit (cat# G1120), DAB substrate kit (cat# DA1010), and goat serum (cat# SL038) were purchased from Solarbio Science & Technology. The DAPI Fluoromount-GTM (cat# 36308ES11) and dihydroethidium (DHE) (cat# 50102ES02) were purchased from Yeasen Biotechnology. The BCA protein assay kit (cat# P0010) was provided by Beyotime Biotechnology. The Omni-ECLTM enhanced pico light chemiluminescence kit and HRP-labeled goat anti-rabbit IgG (H+L) secondary antibody (cat# LF102) were obtained from Epizyme Biomedical Technology. The secondary antibodies of goat anti-rabbit IgG H&L (Alexa Fluor® 488) (cat# ab150077) and goat anti-rabbit IgG H&L (Alexa Fluor® 647) (ab150079) were acquired from Abcam. The primary antibodies against VEGF (cat# AF5131), HIF-1α (cat# AF1009), SOD1 (cat# AF5198), HO1 (cat# AF5393), and NRF2 (cat# AF0639) were purchased from Affinity Biosciences. Primary antibodies anagist Cadherin5 (cat# A0734), MMP9 (cat# A0289), eNOS (cat# A1548), IL-6 (cat# A0286), TNF-α (cat# A0277) and IL-1β (cat# A16288) were purchased from Abclonal Techology. Primary antibody against GAPDH (cat# BA2913) was provided by Boster Biological Technology. All general chemicals were of analytical grade and were purchased from Solarbio Science & Technology.



## 2.3 Random skin flap model

Rats were anesthetized with isoflurane (3% for induction and 2% for maintenance) using gas anesthesia system. Dorsal hair was subsequently removed by shaving and applying depilatory cream. According to the modified McFarlane flap model(24), random skin flaps were established on the dorsal skin of rats. Briefly, a 9 cm × 3 cm rectangular area was drawn on the back of the rats with the midline as the long axis and the line connecting the iliac crests as the short side. Then, the skin was incised along the cranial and lateral lines of the rectangular area, and the bilateral iliac

arteries were exposed and ligated. Afterward, the skin flap was immediately overlaid on the donor bed and sutured with 3-0 nylon single stitches. The skin flap was equally divided into three regions from the distal end to the pedicle: Area I, Area II, and Area III. In the random skin flap model, Area I presents necrosis, Area II suffers from ischemia and tends towards necrosis, while Area III shows normal health(25). To improve the survival rate of the skin flap, the intervention aims to inhibit ischemia and potential necrosis in Area II. Therefore, Area II were selected for examination to evaluate IRI and investigate factors that promote flap survival.

**2.4 Experimental Design and Drug Administration**

A total of 72 rats were randomly separated into three groups: the Control group (n = 24), the MEL group (n = 24), and the MEL+ML385 group (n = 24). According to previous studies(26-28), the MEL group was given an intraperitoneal injection of melatonin (20 mg/kg/d) for 7 consecutive days after the procedure, the Control group was given the same amount of physiological saline, and the MEL + ML385 group was intraperitoneally injected of ML385 (30 mg/kg/d) 30 minutes before melatonin administration. On day 7 after surgery, all animals were euthanized under an overdose of pentobarbital sodium. 12 rats each in the groups were used to evaluate the survival area, blood flow signal intensity, and tissue water content. Furthermore, samples from 6 rats per group were used for western blotting analysis, and samples from another 6 rats per group were used for immunohistochemistry staining, immunofluorescence staining, and HE staining.

**2.5 Macroscopic assessment**

After the procedure, the general condition of random skin flaps were observed daily, including skin color, appearance, texture, and hair growth. High-quality photographs of the skin flaps were taken on postoperative day 7. The necrotic area of the skin flap appeared black-brown, scabbed, tough, and without hair growth, while the surviving area was pink, supple, and had new hair growth. The digital photographs were analyzed with Image-Pro Plus software 6.0 (Media Cybernetics, USA), and the

percentage of survival area was calculated as follows: percentage of survival area (%) = the range of survival area / total area × 100%.

Tissue edema, another marker of skin flap necrosis, was analyzed by the tissue water content. On postoperative day 7 after the procedure, the skin flap tissue samples were weighed and recorded as wet weight. Subsequently, the samples were freeze-dried with a lyophilizer until the sample mass did not lose within two days, and then the samples were weighed and recorded as dry weight. The percentage of tissue water content was calculated as follows: percentage of tissue water content (%) = (wet weight - dry weight) / wet weight × 100%.

**2.6 LDBF imaging**

The blood flow of the skin flap was measured when the rats was under anesthesia and placed in an area delineated by the laser doppler probe. The scanning was repeated three times. The signal intensity of blood flow in the skin flaps were quantified by MoorLDI software 6.1 (Moor Instruments, UK). The perfusion unit (PU) was calculated as the flow velocity multiplied by the concentration of red blood cells, as an indicator of blood perfusion.

**2.7 HE Staining**

Six tissue samples of 1.0 cm × 1.0 cm were acquired from Area II of each flap, and immersed in 4% paraformaldehyde for 24 hours. Then the samples were dehydrated, embedded in paraffin, and cut into 4 μm thick sections. The paraffin sections were stained with HE stain kit. Subsequently, the number of microvessels was counted on six arbitrary fields per section under an optical microscope (Olympus Corporation, Japan), and the mean vessel density was determined as the average value of the number of microvessels per unit area (/mm2).

**2.8 Immunohistochemistry**

4% paraformaldehyde-fixed, paraffin-embedded, 4 μm thick tissue sections were first deparaffinized in xylene and rehydrated in graded ethanol bath. The sections

were incubated in 3% hydrogen peroxide, and antigen retrieval was carried out in 10.2 mM sodium citrate buffer for 20 minutes at 95°C. Sections were then washed with phosphate-buffered saline (PBS) and blocked with 10% goat serum for 10 minutes, and incubated with primary antibodies overnight at 4°C: HIF-1α (1: 200), VEGF (1: 200), TNF-α (1: 200), IL-6 (1: 200), NRF2 (1: 200) and SOD1 (1: 200). Sections were incubated with HRP-labeled secondary antibodies, and developed with a DAB substrate kit, followed with hematoxylin for counterstaining. Images were captured under an Olympus microscope with a DP2-TWAIN image acquisition software system (Olympus Corporation, Japan). Image-Pro Plus software 6.0 (Media Cybernetics, USA) was used to quantify the integral absorbances of HIF-1α, VEGF, TNF-α, IL-6, NRF2 and SOD1 positive vessels. Immunohistochemistry analysis was performed on 6 random fields of 3 sections of each sample.

**2.9 Immunofluorescence and DHE Staining**

The sections were deparaffinized and rehydrated as described above. Following three times of washing, tissue antigen was retrieved using sodium citrate buffer (20 minutes, 95°C). The sections were permeabilized with 0.1% Triton X-100 in PBS, and then incubated in 10% goat serum in PBS for 1 hour at room temperature. Afterward, the sections were incubated overnight at 4°C with the primary antibodies against HIF-1α (1: 200), VEGF (1: 200), TNF-α (1: 200), NRF2 (1: 200), and SOD1 (1: 200). Next, the sections were incubated with secondary antibodies for 1 hour and counterstained with DAPI. Finally, images of positive cells were captured using a fluorescent microscope (Olympus, Japan) and analyzed using Image-Pro Plus software 6.0 (Media Cybernetics, USA). For DHE staining, tissue samples of Area II was dehydrated with 30% sucrose solution after washing with PBS, and then embedded in optimal cutting temperature (OCT) compound. The samples were then frozen at -80°C overnight and cut into 20 μm sections. Next, the tissue slides were incubated with DHE solution in PBS for 30 minutes at room temperature. After washing, the tissue slides were imaged using a fluorescent microscope as above.

### 2.10 Western Blotting

The skin flap samples were lysed with RIPA buffer containing protease inhibitors and PMSF and total protein was collected after centrifugation. The protein concentration was determined by the BCA protein assay kit. Equal amount of protein samples (60 μg) were electrophoresed on 12% sodium dodecyl sulfate-poly-acrylamide gel electrophoresis (SDS-PAGE) gels and transferred to polyvinylidene fluoride (PVDF) membranes. After blocking with 5% nonfat milk (Tris-Buffered Saline with Tween-20 buffer) for 2 hours at room temperature, the membranes were incubated with the corresponding diluted primary antibodies at 4°C overnight: VEGF (1: 1000), MMP9 (1: 1000), Cadherin5 (1: 1000), eNOS (1: 1000), HO1 (1: 1000), SOD1 (1: 1000), TNF-α (1: 1000), IL-6 (1: 1000), IL-1β (1: 1000), NRF2 (1: 1000), GAPDH (1: 1000). Subsequently, the membrane was incubated with secondary antibody at room temperature for 2 hours. After being visualized by the Omni-ECLTM enhanced pico light chemiluminescence kit, the protein bands were analyzed using Image Lab 3.0 software (Bio-Rad, USA).

### 2.11 Statistical Analysis.

Statistical analysis was performed using SPSS version 26 (IBM, USA). The mean and standard deviation (mean ± SD) of the quantitative data were presented. Comparisons between two groups were conducted using independent sample t test, and comparisons of three groups were performed by one-way analysis of variance (ANOVA). A p value of less than 0.05 was considered significant.

## 3. Results

### 3.1 Melatonin Promotes the Survival of Random Skin Flaps.

On postoperative day 7, we evaluated the activity of the random skin flap model by macroscopic assessment, tissue edema, LDBF imaging, and HE staining. Observation of the flap surface and subcutaneous found that the ischemic necrosis area at the distal end of the flap appears dark in color, hard, and shrunken, without hair growth, tissue edema, and severe congestion. In contrast, the surviving area

presents light color, soft, and stretched, with hair growth, with less edema and congestion (Figure 1A, C). Different degrees of ischemic necrosis appeared in Area I and II of the skin flaps in both groups, and the percentage of survival area of the flaps in the MEL group was higher than that in the control group (Figure 1B). Moreover, the percentage of the tissue water content of flaps was significantly decreased in the MEL group compared to the Control group (Figure 1D). The LDBF imaging visualized the vascular network in the flap, and analysis of blood flow showed significantly stronger signal intensity in the MEL group than in the Control group (Figure 1E, F). Besides, the analysis of HE staining revealed that the mean vessel density of flaps in the MEL group was significantly higher compared with that of the Control group (Figure 1G, H). Collectively, these results suggest that melatonin promotes the survival of random skin flaps.

**3.2 Melatonin Promotes Angiogenesis in Random Skin Flaps.**

Improvement in angiogenesis and restoration of blood supply is considered effective in promoting random skin flap survival. Therefore, to verify our hypothesis that melatonin enhances angiogenesis in random skin flaps, we performed immunofluorescence, immunohistochemistry, and western blot analysis. Expression levels of VEGF and HIF1α, two key regulators of hypoxia-induced angiogenesis, were assessed by immunofluorescence staining (Figure 2A, B). The percentage of VEGF and HIF1α positive cells in the MEL group was significantly higher compared with the Control group (Figure 2C, D). Moreover, the expression of VEGF and HIF-1α in the flaps was detected by immunohistochemistry, as shown in Figure 2E. The results were consistent with the immunofluorescence staining, showing that the levels of VEGF and HIF1α in the MEL group were significantly increased compared with the Control group (Figure 2F). The expression levels of angiogenesis-related proteins such as VEGF, MMP9, and Cadherin5 in Area II of random skin flap were assessed by western blot analysis (Figure 2G). The results showed that compared with the Control group, the optical density values of angiogenesis-related proteins in the MEL group were all increased (Figure 2H). Therefore, these results indicate that melatonin

enhances angiogenesis in random skin flaps.

### 3.3 Melatonin Reduces Oxidative Stress in Random Skin Flaps.

Oxidative stress, especially the accumulation of ROS, plays an important role in ischemia-reperfusion injury of skin flaps. Therefore, we hypothesized that melatonin promotes skin flap survival by reducing oxidative stress. To confirm our hypothesis, we assessed the level of ROS and the expression of antioxidant proteins such as SOD1, HO1, and eNOS in Area II of skin flaps. The ROS levels in the flaps were assessed by DHE fluorescence (Figure 3A). Immunofluorescence assays showed that after treatment with melatonin, the optical density value of DHE was significantly lower than that of the Control group (Figure 3C). The western blot analysis and immunofluorescence assays were performed to determine the expression of SOD1 in skin flaps (Figure 3B, E). The results of both western blot and immunofluorescence showed that the expression of SOD1 in the MEL group was markedly increased than that in the Control group (Figure 3D, F). HO1 is acknowledged as cytoprotective enzymes due to its capacity to catabolize cytotoxic free haem and produce antioxidants(29). The results of western blotting showed that the expression of antioxidant proteins (eNOS, HO1, and SOD1) was significantly increased in the MEL group compared with that of the Control group (Figure 3G, H). Therefore, these results suggest that melatonin reduced oxidative stress in random skin flaps.



### 3.4 Melatonin Alleviates Inflammation in Random Skin Flaps.

Next, we investigated whether melatonin has a protective role in the inflammatory response of random skin flaps. First, immunofluorescence staining showed that melatonin significantly decreased the percentage of TNF-α positive cells in the dermal layer of the flaps (Figure 4A, B). Further immunohistochemistry staining likewise showed that the expression levels of TNF-α and IL-6 in the MEL group were lower than those in the Control group (Figure 4C, D). Moreover, western blotting results showed that melatonin administration decreased the expression of inflammatory factors (TNF-α, IL-6, and IL-1β) in the random skin flap model (Figure

4E, F). Thus, these results suggested that melatonin alleviated inflammation by reducing inflammatory cytokines expression.

### 3.5 ML385 Reverses the Pro-survival Effect of Melatonin on Random Skin Flaps.

To investigate the role of NRF2 signaling in the therapeutic effect of melatonin on skin flap survival, we co-administered ML385 (a specific NRF2 inhibitor) with melatonin and evaluated the effects. The results indicated that the percentage of flap survival area in the MEL+ML385 group was significantly lower than that in the MEL group; meanwhile, the survival area was larger in the MEL+ML385 group than that in the Control group (Figure 5A, B). Likewise, co-administration with ML385 aggravated tissue edema of flaps. The percentage of the tissue water content of the MEL+ML385 group was significantly higher than that of the MEL group (Figure 5C, D). Moreover, the LDBF analysis showed that the signal intensity of blood flow of the MEL+ML385 group was significantly lower than that of the MEL group (Figure 5E, F). Besides, the analysis of HE staining demonstrated that the mean vessel density of flaps in the MEL+ML385 group was significantly decreased compared with that in the MEL group (Figure 5G, H). Altogether, these results suggested that ML385 significantly reversed the positive effect of melatonin on random skin flap survival, which may be associated with the activation of the NRF2 signaling pathway by melatonin.



### 3.6 Melatonin Promotes Angiogenesis, Reduces Oxidative Stress, and Alleviates Inflammation by activating NRF2.

First, the results of immunohistochemistry and western blotting analysis showed that the level of NRF2 in the MEL+ML385 group was significantly lower than that in the MEL group (Figure 6B, D, G, H). In addition, immunofluorescence staining results showed that the percentage of NRF2-positive cells in the flaps was significantly reduced in the MEL+ML385 group (Figure 6A, C). These results indicated that NRF2 in melatonin-treated random skin flaps was successfully inhibited by ML385.

Subsequently, we assessed whether co-administration with ML385 affected the efficacy of melatonin in angiogenesis, oxidative stress, and inflammatory responses. The expression of proteins associated with angiogenesis, oxidative stress, and inflammation was determined using western blotting, immunohistochemistry, and immunofluorescence in random skin flaps. Firstly, Immunofluorescence staining showed that compared with the MEL group, the percentage of VEGF and SOD1 positive cells was significantly decreased, while the percentage of TNF-α positive cells and ROS level were significantly increased in the MEL+ML385 group (Figure 6A, C, E, F). Moreover, immunohistochemistry staining showed that co-administration with ML385 significantly decreased the expression of VEGF and increased the expression of TNF-α (Figure 6B, D). Similarly, the quantification results of western blotting showed that compared with the MEL group, the levels of VEGF, SOD1, and HO1 were significantly decreased, and the levels of inflammatory cytokines (TNF-a and IL-6) were significantly increased in the MEL+ML385 group (Figure 6G, H). In summary, our findings suggested that melatonin activates NRF2 in random skin flaps, which is the primary mechanism by which melatonin promotes angiogenesis, reduces oxidative stress, alleviates inflammation, and ultimately improves the survival of random skin flaps.

## 4. Discussion

Among the skin flaps currently used in clinical practice, random skin flaps have become a common transplantation technique for repairing skin defects in plastic surgery because of their convenient sampling and similar color and texture to the skin at the wound site. The vascular supply of the random skin flap is through the dermal-subdermal plexus(30). Therefore, the site and longitudinal axis of the donor flap are not restricted by the axial vessels. However, ischemic necrosis of random skin flaps is a common complication, especially in the distal portion of the flap. The main causes of ischemic necrosis of distal skin flaps are insufficient blood supply and ischemia-reperfusion injury. Oxidative stress and inflammatory response are two important mechanisms of ischemia-reperfusion injury, leading to further tissue damage or

necrosis. The ischemic necrosis of distal flaps is an important reason for the poor prognosis of random skin flaps, including affecting the function and appearance of organs, limiting clinical application, prolonging hospital stay, increasing the economic burden of patients(31). Therefore, it is still of clinical significance to study strategies to improve the survival rate of random skin flaps.

Melatonin, an endogenous hormone secreted by the pineal gland, has the functions of regulating cell proliferation, differentiation, metastasis, metabolism, and apoptosis. In different pathophysiological processes, the effect of melatonin on angiogenesis is different, which may be related to its specific regulation mechanism of melatonin receptor and VEGF. On the one hand, previous studies have shown that melatonin inhibits angiogenesis by suppressing HIF-1α-VEGF pathway in vascular endothelial cells under hypoxia(32, 33). On the other hand, it has been reported that melatonin promotes BMSC-mediated angiogenesis in bone defects(20) and MMP2-mediated angiogenesis in gastric ulcers by upregulating the level of VEGF(21). Furthermore, melatonin has been reported to attenuate inflammation, oxidative stress, and apoptosis by activating NRF2 signaling pathway(34-36). In addition, there are numerous studies reported the protective effect of melatonin against ischemia-reperfusion injury in brain, heart, liver, and others(37-39). Therefore, we hypothesized that melatonin may reduce ischemic necrosis in random skin flaps, which was validated in our current work. Our study found that the survival area and tissue edema of random skin flap improved, indicating that melatonin effectively promotes random skin flap survival.

Previous studies have shown that promoting angiogenesis is critical for flap survival(40). Angiogenesis is a complex process of forming new blood vessels by sprouting endothelial cells from pre-existing blood vessels, including proliferation, differentiation, guided migration, and quiescence of endothelial cells(41). VEGF serves as an initial angiogenic signal that promotes proliferation, migration and sprouting of endothelial cells, and increases vascular permeability(42). HIF-1α initiates broad transcriptional responses to promote angiogenesis, through the upregulation of angiogenic factors such as VEGF(43). In our study, we found that

390 melatonin increased signal density of blood flow in flap and improved the vessel
391 density in the dermis. Our results also showed increased expressions of VEGF, HIF-
392 1α, MMP9, and Cadherin5 proteins with melatonin treatment, suggesting that
393 melatonin promoted angiogenesis in random pattern skin flap. Our study found that
394 melatonin-induced angiogenesis stimulates the viability of random skin flaps.
395 Ischemia-reperfusion injury is an important cause of flap necrosis, manifested by
396 the accumulation of ROS, inflammation, and apoptosis. High levels of ROS lead to
397 oxidative stress, cellular damage and ultimately cell death. Previous studies have
398 shown that melatonin acts as an antioxidant to thwart oxidative damage in a
399 remarkable array of ways(44). Melatonin can not only directly scavenge a variety of
400 ROS and reactive nitrogen species, but also indirectly stimulate antioxidant enzymes
401 while inhibiting the activity of pro-oxidative enzymes. Therefore, we hypothesized
402 that melatonin may promote random skin flap survival by inhibiting oxidative stress.
403 SOD1 is an antioxidant enzyme that catalyzes the transformation of superoxide to
404 hydrogen peroxide(45). HO1 is a subtype of heme oxygenase with potent antioxidant
405 activity. eNOS is an enzyme with antioxidant activity. Measurement of intracellular
406 ROS was performed using DHE staining. In our study, we observed that melatonin
407 increased the levels of anti-oxidative stress-related proteins SOD1, HO1, and eNOS
408 and decreased the level of ROS in random skin flaps. These results suggest that
409 melatonin promotes random skin flap survival by alleviating oxidative stress.
410 Inflammation has been implicated as one of the main responses in random skin
411 flap ischemia-reperfusion injury and blocking various aspects of the inflammatory
412 cascade has been demonstrated to alleviate ischemia-reperfusion injury. Therefore, we
413 hypothesized that melatonin may promote random skin flap survival by suppressing
414 inflammatory response. It was previously reported that melatonin ameliorated the
415 progression of atherosclerosis through attenuating NLRP3 inflammasome
416 activation(46). Another study confirmed that melatonin effectively reduced the
417 expression of pro-inflammatory factors TNF-α and IL-8 in severe osteoarthritis(47).
418 In our study, using western blotting, immunohistochemistry, and
419 immunofluorescence, we observed that melatonin treatment reduced the levels of pro-

420 inflammatory cytokines including TNF-α, IL-6, and IL-1β. These results suggest that
421 melatonin promotes random skin flap survival by alleviating inflammatory response.
422 ML385 is a specific NRF2 inhibitor which leads to a significant reduction in the
423 expression of NRF2 and downstream target genes(48). Furthermore, NRF2 signaling
424 acts as a master regulator of antioxidant stress, regulating the expression of
425 antioxidant genes and phase II detoxification enzymes such as HO1, which remove
426 cytotoxic ROS to counteract oxidative damage(49). The present study demonstrates
427 that ML385 inhibits NRF2, thereby reversing melatonin-mediated promotion of skin
428 flap viability and reduction of tissue edema. Furthermore, ML385 treatment reduced
429 the levels of SOD1, HO1 and ROS in melatonin-treated flaps. These findings imply
430 that melatonin alleviates oxidative stress in random skin flaps by activating NRF2. It
431 has been reported that NRF2 suppresses macrophage inflammatory response via
432 blocking proinflammatory cytokine transcription(50). Our study found that ML385
433 treatment suppressed the levels of TNF-α and IL-6 in random skin flaps treated with
434 melatonin. This finding implies that melatonin alleviates inflammation in random skin
435 flap through NRF2 activation. Previous studies have shown that NRF2 contributes to
436 angiogenesis potential of endothelial cells(51). NRF2-inhibited cancer cells under
437 hypoxic conditions results in the inability to accumulate HIF-1α protein, possibly due
438 to reduced mitochondrial oxygen consumption(52). In the present study, ML385
439 reduced the vessel density and vascular network distribution and inhibited the
440 expression of VEGF in melatonin-treated flaps. This suggests that ML385 may
441 attenuate angiogenesis by inhibiting NRF2. Therefore, our current research findings
442 indicate that melatonin can activate NRF2 and facilitate its nuclear translocation,
443 thereby enhancing the expression of antioxidant enzymes. The upregulation of these
444 antioxidant enzymes inhibits oxidative stress and inflammation in random skin flaps,
445 while also promoting angiogenesis.
446 Our study has some limitations that need to be addressed in future studies. First,
447 our results are based on in vivo experiments and no in vitro experiments were
448 performed to determine other mechanisms by which melatonin enhances random skin
449 flap survival. Second, this study used an effective dose of melatonin rather than

concentration gradient to select an optimal dose. In addition, it is unknown whether the effects of melatonin on angiogenesis are affected by other conditions, such as drug concentration, timing, and duration of management. Whether other pathways participate in the antiangiogenic effect of melatonin requires further investigation. Furthermore, stem cell-based tissue engineering therapies are considered promising strategies for tissue regeneration, and future research can further explore the role of mesenchymal stem cells in skin tissue regeneration(53, 54). Nevertheless, this study presents the benefit of melatonin for random skin flaps and lays the foundation for further research.

## 5. Conclussion

In conclusion, our study demonstrated that the melatonin promotes the survival of random skin flaps by activating NRF2 signaling pathway to promote angiogenesis, inhibit oxidative stress and inflammation. The results showed that inhibition of NRF2 reverses the beneficial effect of melatonin on random skin flaps. Activation of NRF2 pathway may reduce ROS levels, thereby suppressing inflammation. Therefore, melatonin treatment enhances skin flap viability. The present work provides an important basis for evaluating the beneficial effects of on random skin flaps. Further studies should be conducted to better understand the potential clinical utility of melatonin.



**Acknowledgments**

Funding: This study was supported by the Wenzhou Basic Scientific Research Project (NO. Y20210046).

**Footnote**

**Reporting Checklist:** The authors have completed the Original Article reporting checklist.

**Conflict of interest:** All authors have completed the ICMJE uniform disclosure form. The authors have no conflicts of interest to declare.

**Ethical Statement:** The authors are accountable for all aspects of the work in ensuring that questions related to the accuracy or integrity of any part of the work are appropriately investigated and resolved. Experiments were performed under a project license (NO.: xmsq2022-0057) granted by ethics board of Wenzhou Medical University, in compliance with China national or institutional guidelines for the care and use of animals.

**Abbreviation**

ROS: Reactive oxygen species
IRI: Ischemia-reperfusion injury
MEL: Melatonin
LDBF: Laser doppler blood flow
HE: Hematoxylin-eosin
NRF2: Nuclear factor erythroid 2 related factor 2
KEAP1: Kelch-like ECH-associated protein 1
MAFG: Musculoaponeurotic Fibrosarcoma Oncogene Homologue G
DHE: Dihydroethidium
VEGF: Vascular endothelial growth factor
HIF-1α: Hypoxia inducible factor 1α
SOD1: Superoxide dismutase 1
HO1: Heme oxygenase 1
MMP9: Matrix metalloproteinase 9
eNOS: Endothelial NOS
IL-6: Interleukin 6
TNF-α: Tumour necrosis factor α

IL-1β: Interleukin 1β

GAPDH: Glyceraldehyde-3-phosphate dehydrogenase

MT: Melatonin receptor

## References

[1] Norman G, Wong JK, Amin K, et al. Reconstructive surgery for treating pressure ulcers. Cochrane Database Syst Rev. 2022; 10(10):CD012032.

[2] Ogawa R. Surgery for scar revision and reduction: from primary closure to flap surgery. Burns Trauma. 2019; 7:7.

[3] van den Heuvel MG, Buurman WA, Bast A, et al. Review: Ischaemia-reperfusion injury in flap surgery. J Plast Reconstr Aesthet Surg. 2009; 62(6):721-6.

[4] Chouchani ET, Pell VR, James AM, et al. A Unifying Mechanism for Mitochondrial Superoxide Production during Ischemia-Reperfusion Injury. Cell Metab. 2016; 23(2):254-63.

[5] Hou R, Lu T, Gao W, et al. Prussian Blue Nanozyme Promotes the Survival Rate of Skin Flaps by Maintaining a Normal Microenvironment. ACS Nano. 2022; 16(6):9559-71.

[6] Ordeghan AN, Khayatan D, Saki MR, et al. The Wound Healing Effect of Nanoclay, Collagen, and Tadalafil in Diabetic Rats: An In Vivo Study. Advances in Materials Science and Engineering. 2022; 2022:9222003.

[7] Tavakolizadeh M, Pourjavadi A, Ansari M, et al. An environmentally friendly wound dressing based on a self-healing, extensible and compressible antibacterial hydrogel. Green Chemistry. 2021; 23(3):1312-29.

[8] Yamamoto M, Kensler TW, Motohashi H. The KEAP1-NRF2 System: a Thiol-Based Sensor-Effector Apparatus for Maintaining Redox Homeostasis. Physiol Rev. 2018; 98(3):1169-203.

[9] Lu MC, Ji JA, Jiang ZY, et al. The Keap1-Nrf2-ARE Pathway As a Potential Preventive and Therapeutic Target: An Update. Med Res Rev. 2016; 36(5):924-63.

[10] Singh A, Venkannagari S, Oh KH, et al. Small Molecule Inhibitor of NRF2 Selectively Intervenes Therapeutic Resistance in KEAP1-Deficient NSCLC Tumors. ACS Chem Biol. 2016; 11(11):3214-25.

[11] Cen M, Ouyang W, Zhang W, et al. MitoQ protects against hyperpermeability of endothelium barrier in acute lung injury via a Nrf2-dependent mechanism. Redox Biol. 2021; 41:101936.

[12] Li H, Jiang R, Lou L, et al. Formononetin Improves the Survival of Random Skin Flaps Through PI3K/Akt-Mediated Nrf2 Antioxidant Defense System. Front Pharmacol. 2022; 13:901498.

[13] Madebo MP, Zheng Y, Jin P. Melatonin-mediated postharvest quality and antioxidant properties of fresh fruits: A comprehensive meta-analysis. Compr Rev Food Sci Food Saf. 2022; 21(4):3205-26.

[14] NaveenKumar SK, Hemshekhar M, Jagadish S, et al. Melatonin restores neutrophil functions and prevents apoptosis amid dysfunctional glutathione redox system. J Pineal Res. 2020; 69(3):e12676.
[15] Ma N, Zhang J, Reiter RJ, et al. Melatonin mediates mucosal immune cells, microbial metabolism, and rhythm crosstalk: A therapeutic target to reduce intestinal inflammation. Med Res Rev. 2020; 40(2):606-32.
[16] Golabchi A, Wu B, Li X, et al. Melatonin improves quality and longevity of chronic neural recording. Biomaterials. 2018; 180:225-39.
[17] Sato K, Meng F, Francis H, et al. Melatonin and circadian rhythms in liver diseases: Functional roles and potential therapies. J Pineal Res. 2020; 68(3):e12639.
[18] Kong X, Gao R, Wang Z, et al. Melatonin: A Potential Therapeutic Option for Breast Cancer. Trends Endocrinol Metab. 2020; 31(11):859-71.
[19] Hu W, Liang JW, Liao S, et al. Melatonin attenuates radiation-induced cortical bone-derived stem cells injury and enhances bone repair in postradiation femoral defect model. Mil Med Res. 2021; 8(1):61.
[20] Zheng S, Zhou C, Yang H, et al. Melatonin Accelerates Osteoporotic Bone Defect Repair by Promoting Osteogenesis-Angiogenesis Coupling. Front Endocrinol (Lausanne). 2022; 13:826660.
[21] Ganguly K, Sharma AV, Reiter RJ, et al. Melatonin promotes angiogenesis during protection and healing of indomethacin-induced gastric ulcer: role of matrix metaloproteinase-2. J Pineal Res. 2010; 49(2):130-40.
[22] Zitkute V, Kvietkauskas M, Maskoliunaite V, et al. Melatonin and Glycine Reduce Uterus Ischemia/Reperfusion Injury in a Rat Model of Warm Ischemia. Int J Mol Sci. 2021; 22(16).
[23] Qi X, Wang J. Melatonin improves mitochondrial biogenesis through the AMPK/PGC1alpha pathway to attenuate ischemia/reperfusion-induced myocardial damage. Aging (Albany NY). 2020; 12(8):7299-312.
[24] Lee JH, You HJ, Lee TY, et al. Current Status of Experimental Animal Skin Flap Models: Ischemic Preconditioning and Molecular Factors. Int J Mol Sci. 2022; 23(9).
[25] Zhou K, Chen H, Lin J, et al. FGF21 augments autophagy in random-pattern skin flaps via AMPK signaling pathways and improves tissue survival. Cell Death Dis. 2019; 10(12):872.
[26] Lee FY, Sun CK, Sung PH, et al. Daily melatonin protects the endothelial lineage and functional integrity against the aging process, oxidative stress, and toxic environment and restores blood flow in critical limb ischemia area in mice. J Pineal Res. 2018; 65(2):e12489.
[27] Liu Z, Gan L, Luo D, et al. Melatonin promotes circadian rhythm-induced proliferation through Clock/histone deacetylase 3/c-Myc interaction in mouse adipose tissue. J Pineal Res. 2017; 62(4).
[28] Xu C, Liu Y, Yang J, et al. Effects of berbamine against myocardial ischemia/reperfusion injury: Activation of the 5' adenosine monophosphate-activated protein kinase/nuclear factor erythroid 2-related factor pathway and changes in the mitochondrial state. Biofactors. 2022; 48(3):651-64.
[29] Campbell NK, Fitzgerald HK, Dunne A. Regulation of inflammation by the

595 antioxidant haem oxygenase 1. Nat Rev Immunol. 2021; 21(7):411-25.
596 [30] Honrado CP, Murakami CS. Wound healing and physiology of skin flaps. Facial
597 Plast Surg Clin North Am. 2005; 13(2):203-14, v.
598 [31] Zheng YH, Yin LQ, Xu HK, et al. Non-invasive physical therapy as salvage
599 measure for ischemic skin flap: A literature review. World J Clin Cases. 2021;
600 9(14):3227-37.
601 [32] Cheng J, Yang HL, Gu CJ, et al. Melatonin restricts the viability and
602 angiogenesis of vascular endothelial cells by suppressing HIF-1alpha/ROS/VEGF. Int
603 J Mol Med. 2019; 43(2):945-55.
604 [33] Cerezo AB, Labrador M, Gutierrez A, et al. Anti-VEGF Signalling Mechanism in
605 HUVECs by Melatonin, Serotonin, Hydroxytyrosol and Other Bioactive Compounds.
606 Nutrients. 2019; 11(10).
607 [34] Ali T, Hao Q, Ullah N, et al. Melatonin Act as an Antidepressant via Attenuation
608 of Neuroinflammation by Targeting Sirt1/Nrf2/HO-1 Signaling. Front Mol Neurosci.
609 2020; 13:96.
610 [35] Sun TC, Liu XC, Yang SH, et al. Melatonin Inhibits Oxidative Stress and
611 Apoptosis in Cryopreserved Ovarian Tissues via Nrf2/HO-1 Signaling Pathway. Front
612 Mol Biosci. 2020; 7:163.
613 [36] Yu H, Zhang J, Ji Q, et al. Melatonin alleviates aluminium chloride-induced
614 immunotoxicity by inhibiting oxidative stress and apoptosis associated with the
615 activation of Nrf2 signaling pathway. Ecotoxicol Environ Saf. 2019; 173:131-41.
616 [37] Feng D, Wang B, Wang L, et al. Pre-ischemia melatonin treatment alleviated
617 acute neuronal injury after ischemic stroke by inhibiting endoplasmic reticulum
618 stress-dependent autophagy via PERK and IRE1 signalings. J Pineal Res. 2017; 62(3).
619 [38] Zhang Y, Wang Y, Xu J, et al. Melatonin attenuates myocardial ischemia-
620 reperfusion injury via improving mitochondrial fusion/mitophagy and activating the
621 AMPK-OPA1 signaling pathways. J Pineal Res. 2019; 66(2):e12542.
622 [39] Chen HH, Chen YT, Yang CC, et al. Melatonin pretreatment enhances the
623 therapeutic effects of exogenous mitochondria against hepatic ischemia-reperfusion
624 injury in rats through suppression of mitochondrial permeability transition. J Pineal
625 Res. 2016; 61(1):52-68.
626 [40] Wang X, Yu Y, Yang C, et al. Dynamically Responsive Scaffolds from
627 Microfluidic 3D Printing for Skin Flap Regeneration. Adv Sci (Weinh). 2022;
628 9(22):e2201155.
629 [41] Carmeliet P, Jain RK. Molecular mechanisms and clinical applications of
630 angiogenesis. Nature. 2011; 473(7347):298-307.
631 [42] Wen Z, Shen Y, Berry G, et al. The microvascular niche instructs T cells in large
632 vessel vasculitis via the VEGF-Jagged1-Notch pathway. Sci Transl Med. 2017;
633 9(399).
634 [43] Rankin EB, Giaccia AJ. Hypoxic control of metastasis. Science. 2016;
635 352(6282):175-80.
636 [44] Reiter RJ, Mayo JC, Tan DX, et al. Melatonin as an antioxidant: under promises
637 but over delivers. J Pineal Res. 2016; 61(3):253-78.
638 [45] Montllor-Albalate C, Kim H, Thompson AE, et al. Sod1 integrates oxygen

availability to redox regulate NADPH production and the thiol redoxome. Proc Natl Acad Sci U S A. 2022; 119(1).
[46] Ma S, Chen J, Feng J, et al. Melatonin Ameliorates the Progression of Atherosclerosis via Mitophagy Activation and NLRP3 Inflammasome Inhibition. Oxid Med Cell Longev. 2018; 2018:9286458.
[47] Huang Y, Li Z, Van Dessel J, et al. Effect of platelet-rich plasma on peri-implant trabecular bone volume and architecture: A preclinical micro-CT study in beagle dogs. Clin Oral Implants Res. 2019; 30(12):1190-9.
[48] Xian P, Hei Y, Wang R, et al. Mesenchymal stem cell-derived exosomes as a nanotherapeutic agent for amelioration of inflammation-induced astrocyte alterations in mice. Theranostics. 2019; 9(20):5956-75.
[49] Loboda A, Damulewicz M, Pyza E, et al. Role of Nrf2/HO-1 system in development, oxidative stress response and diseases: an evolutionarily conserved mechanism. Cell Mol Life Sci. 2016; 73(17):3221-47.
[50] Kobayashi EH, Suzuki T, Funayama R, et al. Nrf2 suppresses macrophage inflammatory response by blocking proinflammatory cytokine transcription. Nat Commun. 2016; 7:11624.
[51] Guo Z, Mo Z. Keap1-Nrf2 signaling pathway in angiogenesis and vascular diseases. J Tissue Eng Regen Med. 2020; 14(6):869-83.
[52] Kim TH, Hur EG, Kang SJ, et al. NRF2 blockade suppresses colon tumor angiogenesis by inhibiting hypoxia-induced activation of HIF-1alpha. Cancer Res. 2011; 71(6):2260-75.
[53] Hussain A, Tebyaniyan H, Khayatan D. The Role of Epigenetic in Dental and Oral Regenerative Medicine by Different Types of Dental Stem Cells: A Comprehensive Overview. Stem Cells International. 2022; 2022:5304860.
[54] Soudi A, Yazdanian M, Ranjbar R, et al. Role and application of stem cells in dental regeneration: A comprehensive overview. EXCLI Journal. 2021; 20:454-89.



## Figure legends

**Figure 1 Melatonin promotes the survival of random skin flaps.** (A) Digital photographs of random skin flaps in the Control and MEL groups were taken on postoperative day 7 (scale bar: 1.0 cm). (B) Histogram of percentage of survival area on postoperative day 7. (C) Digital photographs of tissue edema in the Control and MEL groups on postoperative day 7 (scale bar: 1.0 cm). (D) Histogram of percentage of tissue water content. (E) Laser Doppler Blood Flow images of flaps showing vascular network and blood supply in the Control and MEL groups on postoperative day 7 (scale bar: 1.0 cm). (F) Histogram of signal intensity of blood flow in flaps. (G) HE staining in Area II of flaps showing the vessels in the Control and MEL groups

678 (original magnification × 200) (scale bar: 50 μm). (H) Histogram of mean vessel
679 density calculated from HE staining. Data are presented as mean ± SD, n = 6 per
680 group. *p < 0.05 and **p < 0.01, vs. Control group.
681
682 **Figure 2 Melatonin promotes angiogenesis in random skin flaps.** (A, B)
683 Immunofluorescence staining for VEGF and HIF-1α positive cells in the dermal layer
684 in the Control and MEL groups (scale bar: 20 μm). (C, D) Histogram showing the
685 percentages of VEGF and HIF-1α positive cells in the Control and MEL groups. (E)
686 Immunohistochemistry for VEGF and HIF-1α expression in the flaps of the Control
687 and MEL groups (original magnification × 200) (scale bar: 50 μm). (F) Histogram
688 showing the intergral absorbance of VEGF and HIF-1α. (G) Western blotting showing
689 the expression of VEGF, MMP9 and Cadherin5 in the Control and MEL groups. (H)
690 Histogram showing the optical density values of VEGF, MMP9 and Cadherin5 in the
691 Control and MEL groups. Data are presented as mean ± SD, n = 6 per group. *p <
692 0.05 and **p < 0.01, vs. Control group.
693
694 **Figure 3 Melatonin reduces oxidative stress in random skin flaps.** (A, B)
695 Immunofluorescence staining for ROS levels and SOD1 positive cells in the dermal
696 layer in the Control and MEL groups (scale bar: 20 μm).(C) Histogram showing the
697 levels of ROS in the Control and MEL groups. (D) Histogram showing the
698 percentages of SOD1 positive cells in the Control and MEL groups. (E)
699 Immunohistochemistry for SOD1 expression in the flaps of the Control and MEL
700 groups (original magnification × 200) (scale bar: 50 μm). (F) Histogram showing the
701 intergral absorbance of SOD1. (G) Western blotting showing the expression of eNOS,
702 HO1 and SOD1 in the Control and MEL groups. (H) Histogram showing the optical
703 density values of eNOS, HO1 and SOD1 in the Control and MEL groups. Data are
704 presented as mean ± SD, n = 6 per group. *p < 0.05 and **p < 0.01, vs. Control
705 group.
706
707 **Figure 4 Melatonin alleviates inflammation in random skin flaps.** (A)

708 Immunofluorescence staining for TNF-α positive cells in the dermal layer in the
709 Control and MEL groups (scale bar: 20 μm). (B) Histogram showing the percentages
710 of TNF-α positive cells in the Control and MEL groups. (C) Immunohistochemistry
711 for TNF-α and IL-6 expression in the flaps of the Control and MEL groups (original
712 magnification × 200) (scale bar: 50 μm). (D) Histogram showing the intergral
713 absorbance of TNF-α and IL-6. (E) Western blotting showing the expression of TNF-
714 α, IL-6 and IL-1β in the Control and MEL groups. (F) Histogram showing the optical
715 density values of TNF-α, IL-6 and IL-1β in the Control and MEL groups. Data are
716 presented as mean ± SD, n = 6 per group. *p < 0.05 and **p < 0.01, vs. Control
717 group.
718
719 **Figure 5 Inhibition of NRF2 signaling reverses the effects of melatonin on**
720 **random skin flap survival.** (A) Digital photographs of flaps in the Control, MEL and
721 MEL+ML385 groups were taken on postoperative day 7 (scale bar: 1.0 cm). (B)
722 Histogram of percentage of survival area on postoperative day 7. (C) Digital
723 photographs of tissue edema in the Control, MEL and MEL+ML385 groups on
724 postoperative day 7 (scale bar: 1.0 cm). (D) Histogram of percentage of tissue water
725 content. (E) Laser Doppler Blood Flow images of flaps showing vascular network and
726 blood supply in the Control, MEL and MEL+ML385 groups on postoperative day 7
727 (scale bar: 1.0 cm). (F) Histogram of signal intensity of blood flow in flaps. (G) HE
728 staining in Area II of flaps showing the vessels in the Control, MEL and
729 MEL+ML385 groups (original magnification × 200) (scale bar: 50 μm). (H)
730 Histogram of mean vessel density calculated from HE staining. Data are presented as
731 mean ± SD, n = 6 per group. *p < 0.05 and **p < 0.01, vs. Control group. #p < 0.05
732 and ##p < 0.01, vs. MEL group.
733
734 **Figure 6 Inhibition of NRF2 signaling reverses the effects of melatonin on**
735 **angiogenesis, oxidative stress and inflammation.** (A) Immunofluorescence staining
736 for VEGF, SOD1, TNF-α, NRF2 and HIF-1α positive cells in the dermal layer in the
737 Control, MEL and MEL+ML385 groups (scale bar: 20 μm). (B)

Immunohistochemistry for VEGF, TNF-α and NRF2 expression in the flaps of the Control, MEL and MEL+ML385 groups (original magnification × 200) (scale bar: 50 μm). (C) Histogram showing the percentages of VEGF, SOD1, TNF-α, NRF2 and HIF-1α positive cells in each group. (D) Histogram showing the intergral absorbance of VEGF, TNF-α and NRF2. (E) Immunofluorescence staining for ROS levels in the dermal layer in each groups (scale bar: 20 μm). (F) Histogram showing the levels of ROS in each groups. (G) Western blotting showing the expression of VEGF, SOD1, HO1, TNF-α, IL-6 and NRF2 in each groups. (H) Histogram showing the optical density values of VEGF, SOD1, HO1, TNF-α, IL-6 and NRF2 in each groups. Data are presented as mean ± SD, n = 6 per group. *$p < 0.05$ and **$p < 0.01$, vs. Control group. #$p < 0.05$ and ##$p < 0.01$, vs. MEL group.

**Figure 7 Potential mechanism involved in melatonin treatment on random skin flaps.** Melatonin promotes angiogenesis, inhibits oxidative stress and inflammation by mediating NRF2 signaling pathway and consequently enhances the viability of random skin flaps. In addition, ML385 reserved the beneficial effects of melatonin on flap viability via NRF2 inhibition.

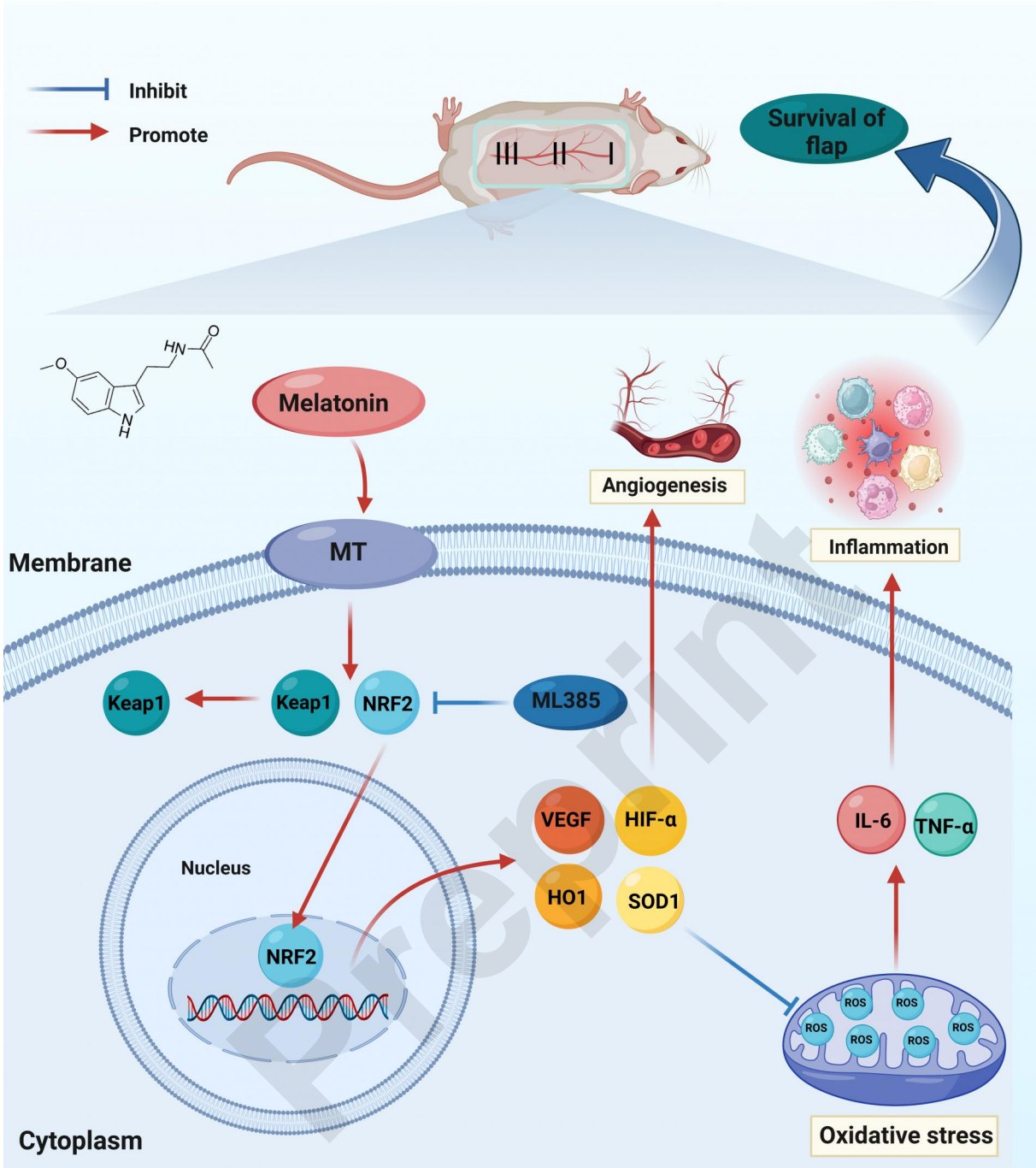
Inhibit
Promote
III
II
I
Survival of flap
Melatonin
Angiogenesis
Inflammation
Membrane
MT
Keap1
Keap1
NRF2
ML385
Nucleus
NRF2
VEGF
HIF-α
HO1
SOD1
IL-6
TNF-α
ROS
Cytoplasm
Oxidative stress

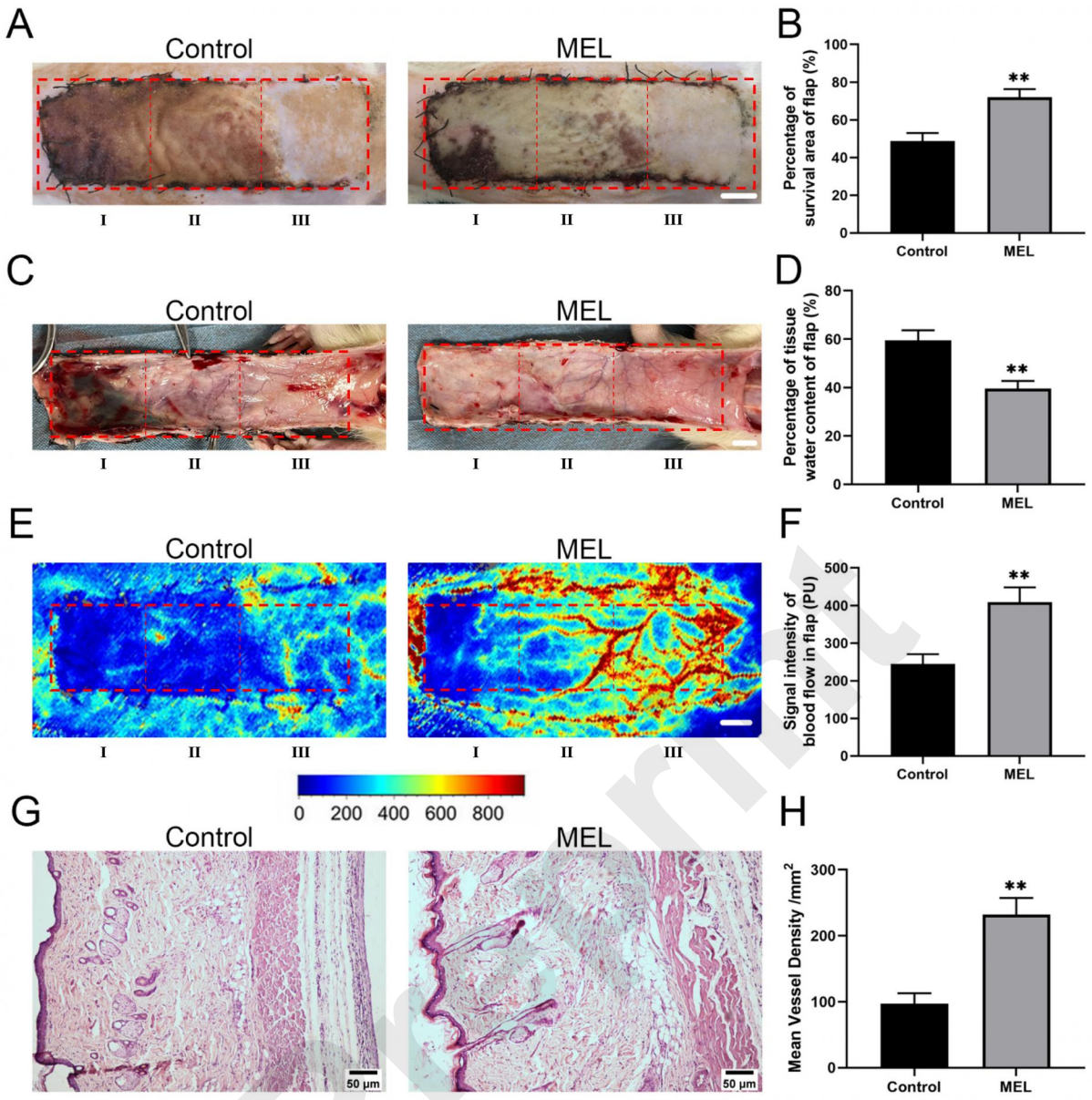


Figure 1 Melatonin promotes the survival of random skin flaps. (A) Digital photographs of random skin flaps in the Control and MEL groups were taken on postoperative day 7 (scale bar: 1.0 cm). (B) Histogram of percentage of survival area on postoperative day 7. (C) Digital photographs of tissue edema in the Control and MEL groups on postoperative day 7 (scale bar: 1.0 cm). (D) Histogram of percentage of tissue water content. (E) Laser Doppler Blood Flow images of flaps showing vascular network and blood supply in the Control and MEL groups on postoperative day 7 (scale bar: 1.0 cm). (F) Histogram of signal intensity of blood flow in flaps. (G) HE staining in Area II of flaps showing the vessels in the Control and MEL groups (original magnification × 200) (scale bar: 50 μm). (H) Histogram of mean vessel density calculated from HE staining. Data are presented as mean ± SD, n = 6 per group. *$p < 0.05$ and **$p < 0.01$, vs. Control group.

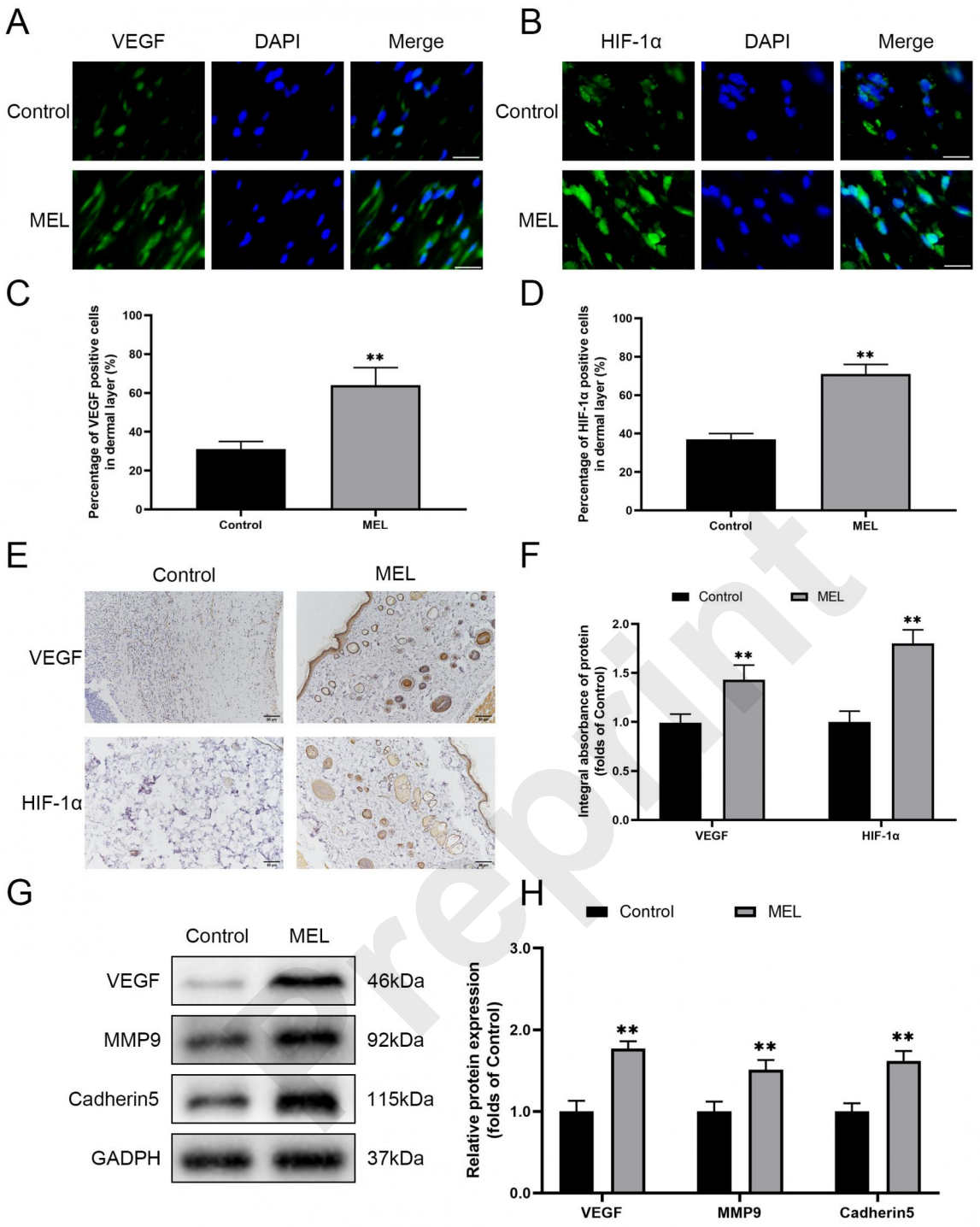


Figure 2 Melatonin promotes angiogenesis in random skin flaps. (A, B) Immunofluorescence staining for VEGF and HIF-1α positive cells in the dermal layer in the Control and MEL groups (scale bar: 20 μm). (C, D) Histogram showing the percentages of VEGF and HIF-1α positive cells in the Control and MEL groups. (E) Immunohistochemistry for VEGF and HIF-1α expression in the flaps of the Control and MEL groups (original magnification ×200) (scale bar: 50 μm). (F) Histogram showing the intergral absorbance of VEGF and HIF-1α. (G) Western blotting showing the expression of VEGF, MMP9 and Cadherin5 in the Control and MEL groups. (H) Histogram showing the optical density values of VEGF, MMP9 and Cadherin5 in the Control and MEL groups. Data are presented as mean ± SD, n=6 per group. *$p < 0.05$ and **$p < 0.01$, vs. Control group.

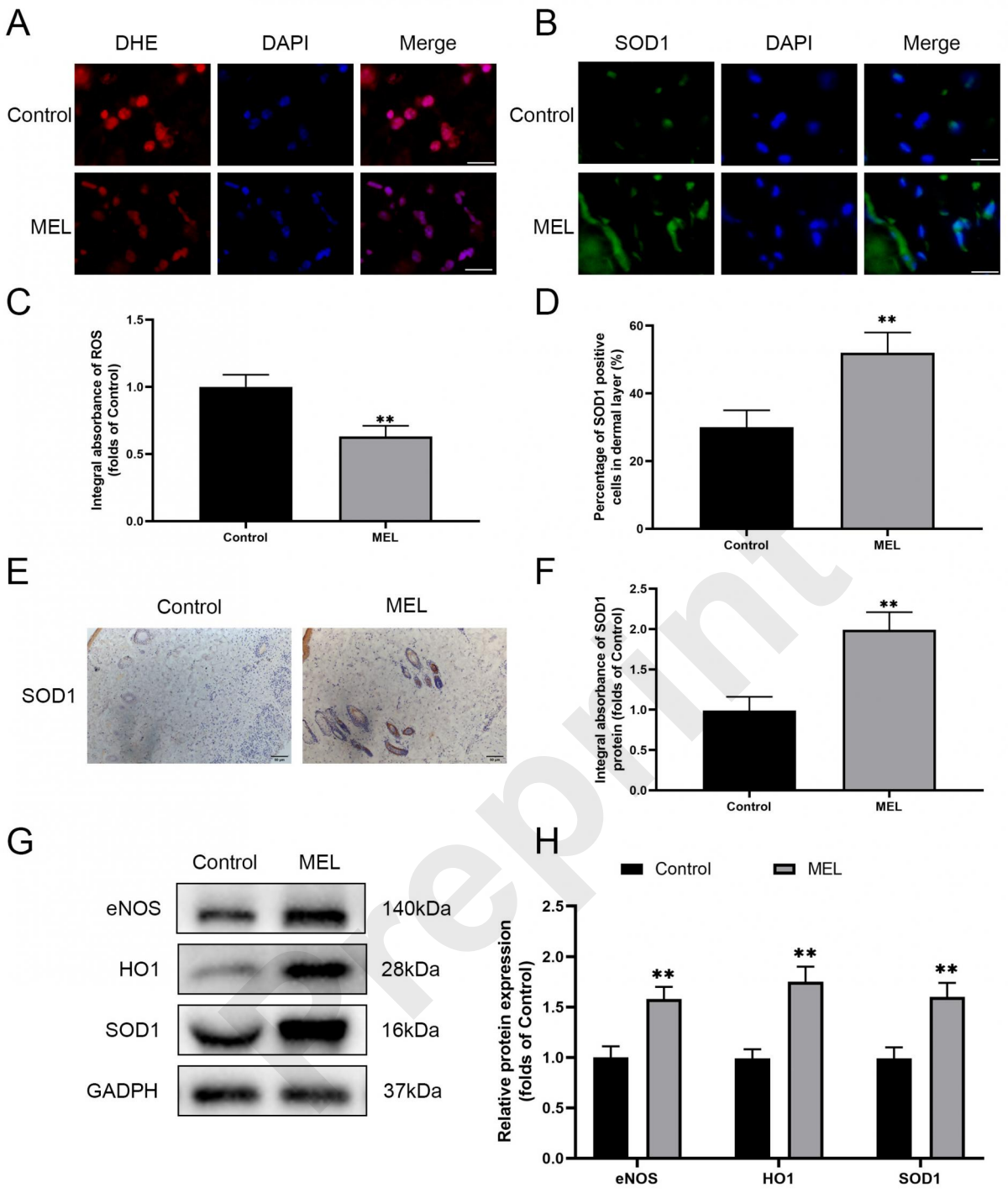


Figure 3 Melatonin reduces oxidative stress in random skin flaps. (A, B) Immunofluorescence staining for ROS levels and SOD1 positive cells in the dermal layer in the Control and MEL groups (scale bar: 20 μm).(C) Histogram showing the levels of ROS in the Control and MEL groups. (D) Histogram showing the percentages of SOD1 positive cells in the Control and MEL groups. (E) Immunohistochemistry for SOD1 expression in the flaps of the Control and MEL groups (original magnification ×200) (scale bar: 50 μm). (F) Histogram showing the intergral absorbance of SOD1. (G) Western blotting showing the expression of eNOS, HO1 and SOD1 in the Control and MEL groups. (H) Histogram showing the optical density values of eNOS, HO1 and SOD1 in the Control and MEL groups. Data are presented as mean ± SD, n=6 per group. *$p < 0.05$ and **$p < 0.01$, vs. Control group.

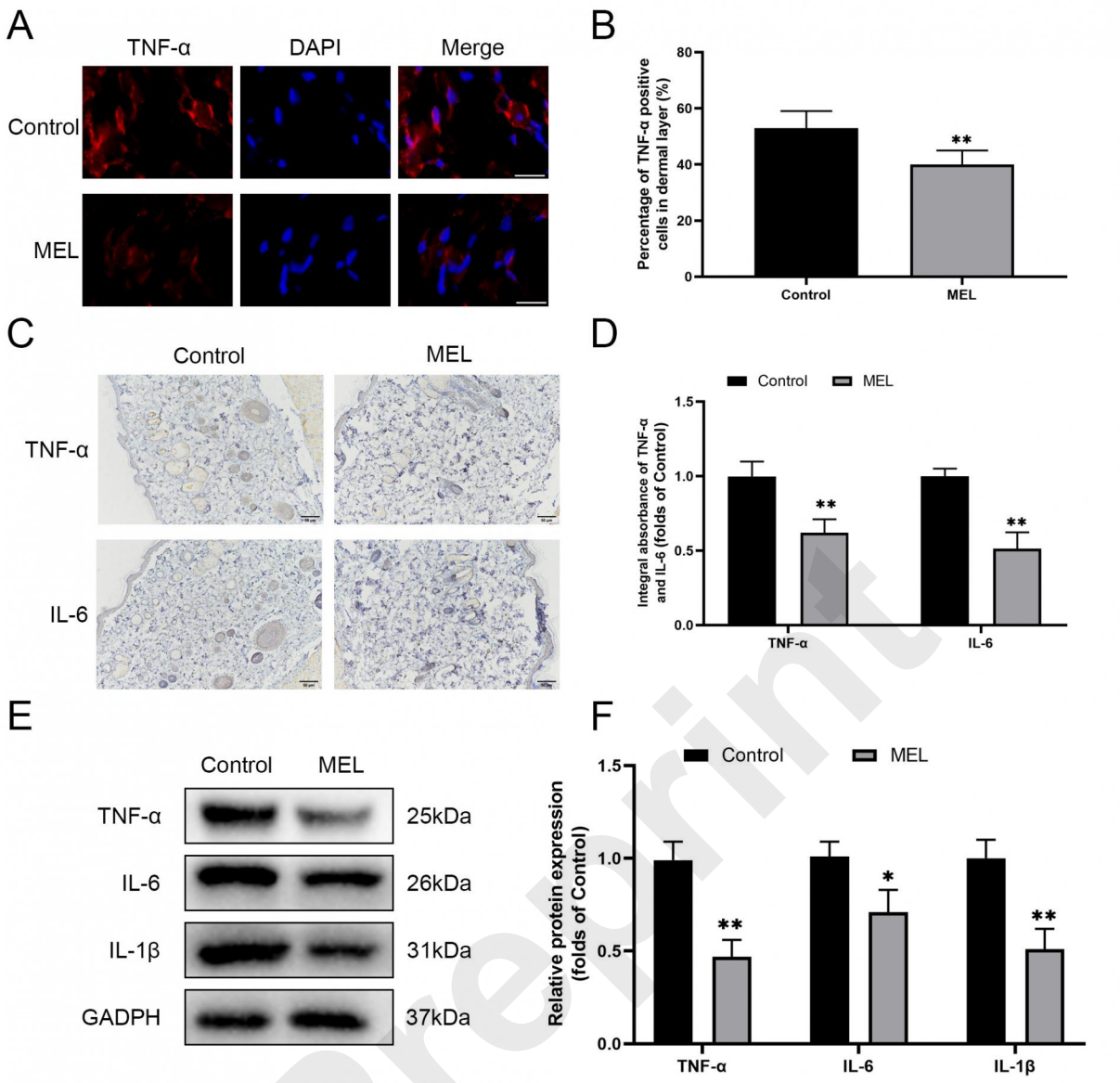


Figure 4 Melatonin alleviates inflammation in random skin flaps. (A) Immunofluorescence staining for TNF-α positive cells in the dermal layer in the Control and MEL groups (scale bar: 20 μm). (B) Histogram showing the percentages of TNF-α positive cells in the Control and MEL groups. (C) Immunohistochemistry for TNF-α and IL-6 expression in the flaps of the Control and MEL groups (original magnification ×200) (scale bar: 50 μm). (D) Histogram showing the intergral absorbance of TNF-α and IL-6. (G) Western blotting showing the expression of TNF-α, IL-6 and IL-1β in the Control and MEL groups. (H) Histogram showing the optical density values of TNF-α, IL-6 and IL-1β in the Control and MEL groups. Data are presented as mean ± SD, n=6 per group. *$p < 0.05$ and **$p < 0.01$, vs. Control group.

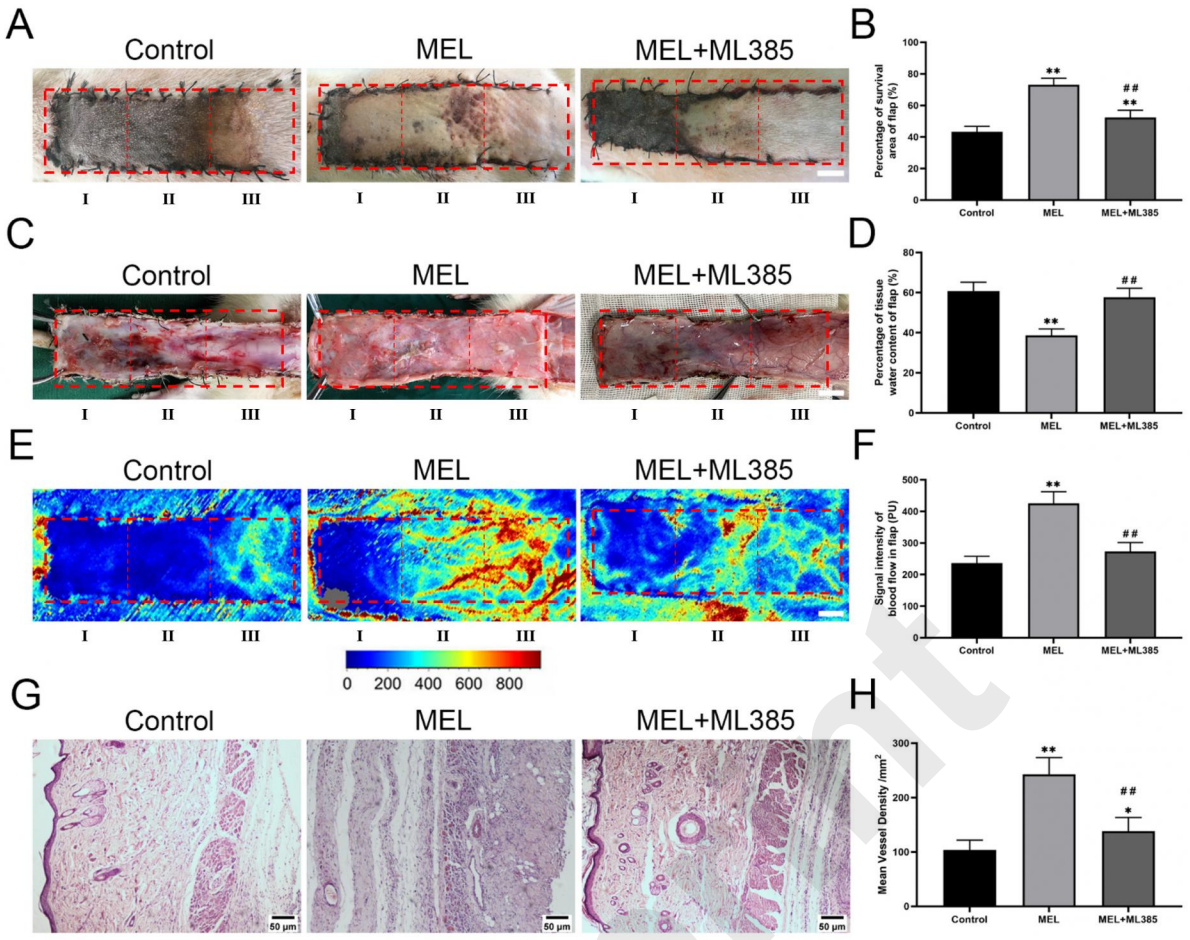


Figure 5 Inhibition of NRF2 signaling reverses the effects of melatonin on random skin flap survival. (A) Digital photographs of flaps in the Control, MEL and MEL+ML385 groups were taken on postoperative day 7 (scale bar: 1.0 cm). (B) Histogram of percentage of survival area on postoperative day 7. (C) Digital photographs of tissue edema in the Control, MEL and MEL+ML385 groups on postoperative day 7 (scale bar: 1.0 cm). (D) Histogram of percentage of tissue water content. (E) Laser Doppler Blood Flow images of flaps showing vascular network and blood supply in the Control, MEL and MEL+ML385 groups on postoperative day 7 (scale bar: 1.0 cm). (F) Histogram of signal intensity of blood flow in flaps. (G) HE staining in Area II of flaps showing the vessels in the Control, MEL and MEL+ML385 groups (original magnification × 200) (scale bar: 50 μm). (H) Histogram of mean vessel density calculated from HE staining. Data are presented as mean ± SD, n = 6 per group. *p < 0.05 and **p < 0.01, vs. Control group. #p < 0.05 and ##p < 0.01, vs. MEL group.

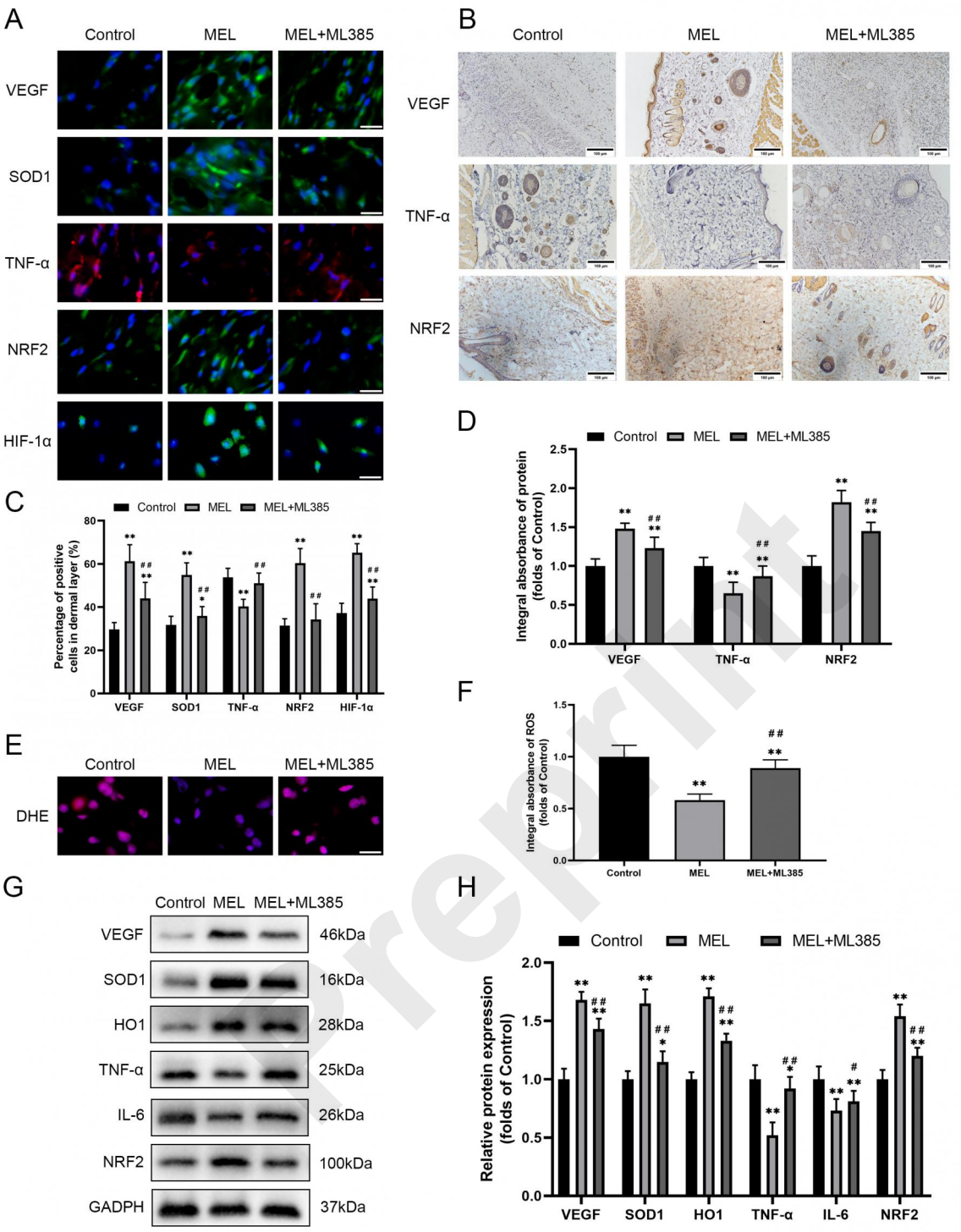


Figure 6 Inhibition of NRF2 signaling reverses the effects of melatonin on angiogenesis, oxidative stress and inflammation. (A) Immunofluorescence staining for VEGF, SOD1, TNF-α, NRF2 and HIF-1α positive cells in the dermal layer in the Control, MEL and MEL+ML385 groups (scale bar: 20 μm). (B) Immunohistochemistry for VEGF, TNF-α and NRF2 expression in the flaps of the Control, MEL and MEL+ML385 groups (original magnification × 200) (scale bar: 50 μm). (C) Histogram showing the percentages of VEGF, SOD1, TNF-α, NRF2 and HIF-1α positive cells in each group. (D) Histogram showing the intergral absorbance of VEGF, TNF-α and NRF2. (E) Immunofluorescence staining for ROS levels in the dermal layer in each groups (scale bar: 20 μm). (F) Histogram showing the levels of ROS in each groups. (G) Western blotting showing the expression of VEGF, SOD1, HO1, TNF-α,

IL-6 and NRF2 in each groups. (H) Histogram showing the optical density values of VEGF, SOD1, HO1, TNF-α, IL-6 and NRF2 in each groups. Data are presented as mean ± SD, n = 6 per group. *$p < 0.05$ and **$p < 0.01$, vs. Control group. #$p < 0.05$ and ##$p < 0.01$, vs. MEL group.